RESISTANCE TO ACID ATTACK OF ALKALI-ACTIVATED BINDERS: SIMPLE NEW TECHNIQUES TO MEASURE SUSCEPTIBILITY

Ana Mellado, Martha Iris Pérez-Ramos, José Monzó, María Victoria Borrachero, Jordi Payá *

Grupo de Investigación en Química de los Materiales (GIQUIMA) Instituto de Ciencia y Tecnología del Hormigón (ICITECH) Universitat Politècnica de València. Camino de Vera s/n E-46022 Valencia (Spain)

*Corresponding author

Abstract

Two rapid tests were developed to evaluate the resistance to acid attack by ordinary Portland cement (OPC) and alkali-activated pastes. Acid neutralisation capacity (ANC) at pH 7, 4 and 2 was monitored with powdered pastes. In parallel, a 'combined-pH assay' with a single sample was used to sequentially assess ANC at different pH values. A mass loss/consumed acid monitoring technique has been also developed in order to assess monolithic samples. The OPC paste showed the most degradation. Among the alkali-activated pastes, those with the lowest calcium content (fly ash and spent-FCC catalyst) had the best performance.

Keywords: Alkali-activated binder; Durability; Acid attack; Acid neutralisation capacity; Mass loss; Consumed acid

1. Introduction

Ordinary Portland cement (OPC) is one of the most used binders in the world. However, their manufacture generates a large amount of carbon dioxide emissions. It needs to be replaced by other more environmentally friendly binders which guarantee durability performance. A promising alternative is the production of other binders such as alkali-activated materials (also called geopolymers).

Geopolymers are formed by a reaction between an aluminosilicate solid material (precursor) and a highly alkaline solution (activating solution) under controlled curing conditions to form a strong dense binding gel [1-4].

Alkali activated binders have either nano-crystalline or amorphous microstructures depending on their reactivity or the percentage of aluminosilicate in the material (precursor), on its nature (mineralogy, fineness), on the alkalinity of the activating solution and on the curing procedure. Most of the previous work in this area used metakaolin, fly ash (FA) and blast furnace slag [5-6]. Other alternative inorganic precursors such as hydrated-carbonated cement, waste glass, spent fluid catalytic cracking catalyst of petroleum (FCC), ceramic waste (CW) or other aluminosilicate materials have been tested to produce alkali-activated materials [7-11].

From the engineering point of view, one of the most important properties in concrete is its durability. As concrete interacts with its external environment, its durability may be threatened, especially by acid attack [12-14] which can reduce its lifetime of service.

The spectrum of aggressive acid media to which concrete can be exposed is broad [12]. Sources usually originate from industrial or agricultural processes, but can also be due to urban activity. Acids can be more or less aggressive towards hydrated compounds: particularly and among others, nitric (HNO_3), hydrochloric (HCl), sulphuric (H_2SO_4) acids are strong acids and

47 behaves very damaging to concrete: hydration products in OPC decompose resulting in a very
48 intense attack.

49 A practical consequence of chemical degradation caused by an acid attack is the gradual
50 weakening of the mechanical strength and solid cohessiveness of concrete. Decay starts by
51 deterioration at the surface of the concrete, resulting in crushing and dropping of material,
52 and continues its destructive progression into the interior portions. As the effects of an acid
53 attack intensify, the strength of the concrete gradually decreases. An acid attack increases
54 total porosity and the percentage of the volume composed of coarse pores as a result of the
55 decomposition and leaching of hydration products.

56 In addition, usually dissolution of the products during an acid attack on hydrated cement
57 results in the formation of a degraded layer which, in many cases, is an easily visible layer,
58 often characterised by a light brown colour marking the front of the attack due to the
59 formation of ferric compounds [15].

60 The severity of an acid attack is significantly dependent on the acid strength. Strong acids (e.g.,
61 nitric or hydrochloric acids) can reach very low pH values even when there is a relatively small
62 amount of them in the solution. The acid attack progress also depends on the nature of the
63 resulting salt: in some cases, insolubility of this salt reduces the inorganic corrosion rate of the
64 matrix [13].

65 The corrosion rate of concrete subjected to acid solutions is a complex process resulting from a
66 combination of dissolution, precipitation and transportation processes. Several factors control
67 this phenomenon of degradation, mainly the chemical composition of the cement, the
68 reactivity of the aggregate and the dosage of the concrete [16].

69 Many authors [17] have claimed that geopolymeric cements are much more resistant to acid
70 attack than OPC. Shi and Stegmann [18] compared the acid resistance of alkali-activated slag

71 and OPC binders when immersed in solutions of nitric acid (pH 3) and in acetic acid (pH 3 and
72 5). They reported that alkali-activated slag binders had lower mass losses than OPC binders.
73 According to these authors, after acid corrosion hardened alkali-activated and OPC binders
74 formed a surface layer whose composition is mainly $SiO_2 \cdot nH_2O$ gel. This layer provides a
75 barrier which prevent further corrosion of the internal, non-corroded cores. However, there is
76 a noticeable difference between the layers formed by alkali-activated slag and OPC. Alkali
77 activated slag produce a protective dense silica gel layer, but hardened OPC leave a porous
78 layer. Differing calcium content (greater in OPC than in alkali-activated slag) could be
79 responsible for this effect.

80 Identical conclusions were obtained by other authors, such as Bakharev *et al*. who
81 demonstrated that when alkali-activated FA concrete was exposed to an acetic acid attack [19]
82 or alkali-activated slag concrete was exposed to acetic or sulfuric acid attacks [20]. In both
83 cases, the resistance of materials was studied by immersion of cylindrical concrete specimens
84 in acid solutions. The durability of alkali-activated materials when exposed to acid solutions
85 was higher than that found for OPC systems.

86 A further study [21] revealed that alkali-activated FA cementitious materials prepared with
87 sodium silicate solution had a lower crystallinity than those prepared with sodium hydroxide
88 activator. With greater crystallinity, alkali-activated binders were more stable in acid
89 environments, such as in sulfuric and acetic acid solutions.

90 Allahverdi and Škvára [22, 23] determined the mechanism of nitric acid attack on hardened
91 pastes of alkali-activated binders based on FA and granulated blast furnace slag. The authors
92 proposed that the mechanism of acid attack consists on: a) dissolution process: sodium and
93 calcium are leached and exchanged by hydronium ions (H_3O^+) from the acid solution; b)
94 electrophilic attack: polymeric Si-O-Al bonds are attacked and aluminium ions are removed
95 from the aluminosilicate framework; c) realignment of chains: the framework vacancies are

mostly re-occupied by silicon atoms and an imperfect highly siliceous framework is formed. The removed aluminium ions (tetrahedral complex) is converted to octahedrally coordinated aluminium, which is distributed in the intra-framework space. Also, volume contraction of the material during the leaching process resulted in the formation of shrinkage cracks.

This paper presents a study of the resistance to nitric acid attack of some alkali-activated pastes prepared from ground granulated blast slag (GGBS), fly ash (FA), spent fluid catalytic cracking catalyst of petroleum (FCC) and ceramic waste (CW) when exposed to nitric acid attack compared to hardened OPC pastes. Samples were stored at controlled pH values of 2, 4 and 7 to calculate the acid neutralisation capacity (ANC) of the powdered materials based the EA NEN 7371:2004 standard [24]. This study outlines a rapid test whereby the weight loss of prismatic specimens submerged in an acid solution (nitric acid, at a constant pH of 2) was measured over time. Also, optical microscopy and scanning electron microscopy (SEM) on samples attacked by nitric acid are presented. We have modelled ANC versus time for the samples at each pH tested in order to predict their behaviour during acid attack. Also equations were modelled to describe mass loss over time for each of the specimens tested.

2. Experimental

To prepare cement pastes, Spanish OPC (CEM I 52.5-R, supplied by Lafarge, Puerto de Sagunto, Spain) that complies with the specifications of EN 196-1 was used. In the preparation of alkali-activated binders, materials were supplied by different companies located in Spain: GGBS (Cementval, Puerto de Sagunto), FA and CW (Balalva, Onda) and FCC (BP Oil, Grao de Castellón). These mineral additions were ground prior to use. Sodium hydroxide pellets (98% purity, Panreac S.A.) and a sodium silicate solution (waterglass; 28% SiO_2, 8% Na_2O and 64% H_2O; Merck) were used to prepare the activating solutions. Calcium hydroxide (95% purity, Panreac S.A.) was used to prepare alkali-activated paste with CW. Table 1 summarises the

121 chemical composition of all materials used as precursors (as determined by X-ray fluorescence)
122 and their mean particle diameter after milling.

123 A reference OPC paste was prepared at a water to cement ratio (w/c) of 0.4.

124 Activating solutions were prepared at least 1 h in advance and allowed to cool to room
125 temperature prior to use. Then they were mixed with each material to prepare the pastes.
126 Table 2 shows the composition of prepared alkali-activated samples. SiO_2/Na_2O is the molar
127 ratio of these oxides in the activating solution. A 5% by mass of $Ca(OH)_2$ was used to replace
128 CW in the CW paste.

129

Oxide (%)	SiO_2	Al_2O_3	Fe_2O_3	CaO	MgO	Na_2O	K_2O	TiO_2	Other	Mean particle diameter (μm)
OPC	20.80	4.60	4.80	65.60	1.20	0.07	1.00	-	1.70	-
GGBS	29.89	10.55	1.29	40.15	7.43	0.87	0.57	0.50	2.58	26
FA	49.91	25.80	13.94	3.84	1.06	-	2.47	-	1.00	21
FCC	47.76	49.26	0.60	0.11	0.17	0.31	0.02	1.22	0.03	17
CW	61.22	18.60	5.02	5.77	1.79	1.49	3.33	0.82	1.08	34

130

131 **Table 1.** Chemical composition and mean particle diameter of materials used.

132 The fresh pastes were cast in prismatic moulds (1 cm x 1 cm x 6 cm), sealed with a plastic film
133 to avoid atmospheric carbonation and stored at 23 ± 2°C with 100% relative humidity for 24 h,
134 except for FA and CW, which needed to be stored in a thermostatically controlled bath at 65 ±
135 2°C for 48 h before demoulding. After demoulding, all specimens were cured at 23 ± 2°C with
136 100% relative humidity for 28 days.

Alkali-activated paste	Water/precursor ratio (g/g)	$[Na^+]$ (mol/kg of solvent)	SiO_2/Na_2O (mol/mol)	Waterglass/precursor ratio (g/g)
GGBS	0.35	7	1.56	0.410
FA	0.30	13	1.12	0.469
FCC	0.4	10	1.17	0.500
CW*	0.4	10	1.17	0.526

137 *In this mix, a 5% by mass of CW was replaced by $Ca(OH)_2$

138 **Table 2.** Mix compositions of alkali-activated pastes.

ANC studies were carried out in an 805 Dosimat Plus automatic titration system (Metrohm) coupled to a Delta-DO9765T pH transmitter (LabProcess). For ANC determination, cured pastes were ground in an agate mortar. One gram of powdered sample (particle size < 125 μm) previously dried at 60°C for 30 min. Samples were stored in a dried atmosphere until ANC tests. Deionized water (50mL) were placed in a beaker and the solid sample was added (the L/S ratio was 50). The sample was magnetically stirred (spinning at 300 revolution per minute). After 10 min of stirring, HNO_3 (0.5 M for pH 7 and 4, and 1 M for pH 2) was added at a flow rate of 4 mL min^{-1} until the desired pH value was reached. The pH values selected for the single-pH assays were 7, 4, and 2. When the solution stabilised at the desired pH, the titration automatically stopped and the volume of acid required to reach this pH value was recorded. The assay was complete when the pH remained constant for longer than 15 min without any acid added by the automated titration system. All tests were carried out in triplicate. The total number of ANC curves measured was 45 (5 pastes x 3 tested pH values x 3 repetitions).

Additionally, a 'combined-pH assay' was carried out in which, after the stabilisation at the first pH value, more acid was added to decrease the pH further (e.g. from 7 to 4, and then from 4 to 2). In this case the sample was not removed from the beaker. HNO_3 (1M) was used as the acid reagent for this 'combined-pH assay'.

The resistance of materials to acid attack was studied by immersion of the prismatic specimens in a HNO_3 solution at a constant pH of 2 with the same device used in the ANC studies. The specimens were suspended in 200 mL of deionised water with the aid of a perforated receptacle. The receptacle held the prismatic specimens while allowing liquid to surround them on all sides. The pH was kept constant by adding 1M HNO_3 with the automated titration system. The volume of acid added was recorded over time, and at predetermined times the specimens were removed from the solution and weighed. The assay was conducted over 120 h. Each paste sample was tested in triplicate.

Deterioration of the surface and subsurface regions of the samples was studied by optical microscopy (LEICA MZ APO) of a freshly fractured specimen and by SEM (JEOL JSM-6300) of samples impregnated with epoxy resin, cut, polished and coated with carbon. Elemental mappings of the polished cross sections were also performed.

3. Results and discussion

3.1. ANC studies

Acid consumption was determined for each sample tested. A single-pH assay was carried out with predetermined pH values.

Experimental results from the ANC test for the OPC and alkali-activated pastes at pH 2, 4 and 7 are shown in Fig. 1. The spent to generate each curve was different for each sample depending on the time required for stabilisation at the selected pH. In general, between 20 and 50 min were required for stabilisation at the selected pH. ANC values were determined in mmol H^+ added per gram of sample (mmol H^+/g).

OPC samples consumed the highest amount of acid. The ANC values for OPC were 15, 18 and 23 mmol H^+/g for pH 7, 4 and 2, respectively. As anticipated, decreases in the pH resulted in more pronounced degradation of the binding matrix, and the acid-base reaction required a larger quantity of acid. Importantly, consumption of acid was necessary to achieve neutralisation at pH 7 because of its reaction with portlandite and the calcium silicate hydrate (C-S-H) gels. Both of these compounds contain high percentages of calcium, suggesting that destruction of hydrated compounds in the OPC matrix could be related to their calcium content.

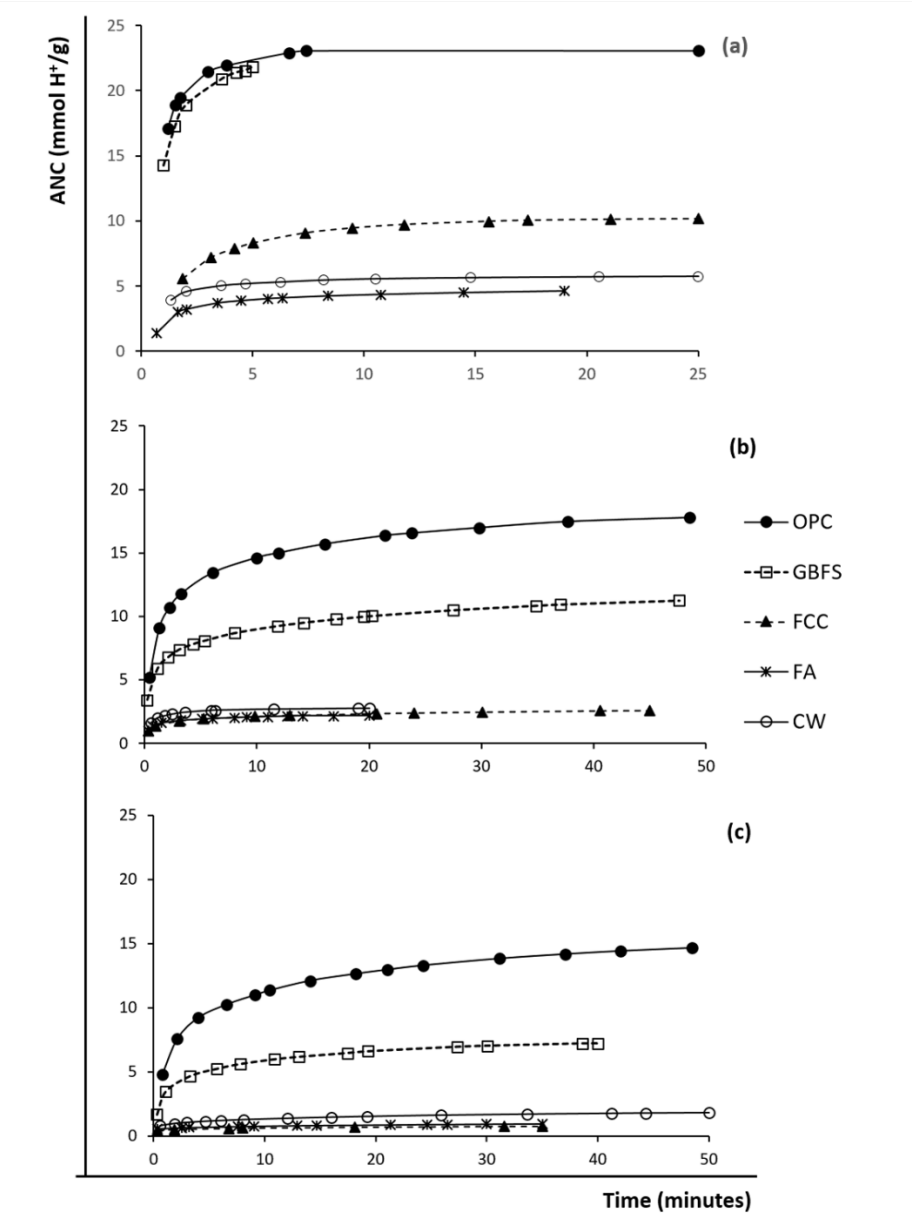

186

187 **Fig. 1** ANC results for the OPC and alkali-activated pastes at **(a)** pH 2, **(b)** pH 4 and **(c)** pH 7.

188

189 GGBS samples showed significant consumption of acid at all three selected pH values. The ANC
190 values for the GGBS samples at pH 7 and pH 4 were significantly lower with respect to the OPC
191 ANC values (approximately 50% less acid was consumed). It was found that alkali activation of
192 GGBS produced mainly calcium aluminosilicate hydrate (C-A-S-H) gels. Apparently, these gels

were more resistant to acid attack at these pH values. However, for pH 2 the ANC values were similar for OPC and GGBS, suggesting that the acid resistance of both systems was similar.

By contrast, FA, FCC and CW systems had significantly lower ANC values, requiring less than 3 mmol H^+/g to obtain pH 7 and pH 4. At pH 2, FA and CW had ANC values less than 6 mmol H^+/g, while FCC was higher at 10 mmol H^+/g. The common characteristic of these systems is their low calcium content. It is well-known that alkali activation of low calcium systems produces sodium aluminosilicate hydrate (N-A-S-H) gels, and the behaviour observed in our experiments suggests that these type of gels have good stability during acid attack.

With the exception of FCC, ANC values were directly correlated to the Ca content of the samples. Higher Ca content in the samples led to higher ANC values. FCC samples behaved differently, especially in the tests at pH 2. The reason for this behaviour could be due to the different curing conditions used to prepare this sample. While the FCC sample was cured at room temperature, FA and CW samples (which have a higher percentage of Ca than FCC) were cured at 65°C, which causes chemical reactions to progress to a greater extent and the high curing temperature stabilised the formed N-A-S-H gel to a greater extent. Thus there were fewer available alkaline ions in these samples than in the FCC sample.

The fit of equations to ANC versus time data for the samples at each different pH are given in Table 3. The time range over which the equations fit the data is indicated. Separate equations were required to fit two different time intervals for the FA, FCC and CW samples at pH 2. The shape of the curves made it impossible to fit a single equation for these samples, which we attribute to the low Ca content in these materials. While samples with high Ca content (OPC and GGBS) were neutralised continuously throughout the titration, samples with low levels of Ca (FA, FCC and CW) were neutralised quickly (during the first 10 minutes) and remained stable.

	pH	Equation	Time interval (minutes)
OPC	2	$y = 3.0217 \ln x + 17.464$	1.20 – 8.00
	4	$y = 2.5975 \ln x + 8.338$	0.23 – 50.00
	7	$y = 2.2685 \ln x + 5.9196$	0.75 – 50.00
GGBS	2	$y = 4.3719 \ln x + 15.097$	0.98 – 5.00
	4	$y = 1.4513 \ln x + 5.6584$	0.23 – 50.00
	7	$y = 1.1178 \ln x + 3.2651$	0.30 – 40.00
FA	2*	$y = 1.0853 \ln x + 2.1814$	0.67 – 8.00
		$y = 0.3323 \ln x + 3.5924$	8.00 – 20.00
	4	$y = 0.2858 \ln x + 1.3924$	0.37 – 20.00
	7	$y = 0.0875 \ln x + 0.609$	0.38 – 35.00
FCC	2*	$y = 2.3663 \ln x + 4.3386$	1.87 – 9.00
		$y = 1.1248 \ln x + 6.7595$	9.00 – 25.00
	4	$y = 0.3335 \ln x + 1.3176$	0.38 – 45.00
	7	$y = 0.0707 \ln x + 0.4781$	0.33 – 35.00
CW	2*	$y = 1.1279 \ln x + 3.1759$	1.33 – 10.00
		$y = 0.2176 \ln x + 5.0421$	10.00 – 25.00
	4	$y = 0.2916 \ln x + 1.9672$	0.58 – 20.00
	7	$y = 0.246 \ln x + 0.8106$	0.60 – 50.00

Table 3. Fitting equations of ANC versus time (y is ANC in mmol H^+/g and x is time in min). * The shape of these curves makes them impossible to fit with a single equation, thus two equations were used to fit the data in the noted time intervals.

To determine the ANC value of a sample at different pH values in a single experiment rather than making three ANC measurements at three different pH values, we outline a new method called 'combined-pH assay'. This assay involves determining the ANC of a sample at different pH values in the same experiment.

The 'combined-pH assay' begins at pH 7. Once a constant ANC value is reached for a particular sample at pH 7, pH 4 is selected allowing the automated acid titration to continue. Similarly, once the ANC value stabilises at pH 4, pH 2 is selected and the titration continues to the end of the experiment. Thus, the ANC of a sample can be determined in a single test. Fig. 2 shows the results from the 'combined-pH assay' for GGBS and FCC samples displayed alongside the results from the 'single-pH assay'.

We applied the 'combined-pH assay' to all other sample types and compared the results to ANC values determined in the 'single-pH assay'. Table 4 shows the difference (in percentage) between the ANC results obtained from the 'combined-pH assay' and the 'single-pH assay', with respect to the 'single-pH assay' results, as calculated by Equation 1:

$$\frac{\mathrm{ANC_{combined}} - \mathrm{ANC_{single}}}{\mathrm{ANC_{single}}} * 100 \qquad \textit{(Eq.1)}$$

	pH 7			pH 4			pH 2		
	C (std)	S (std)	%	C (std)	S (std)	%	C (std)	S (std)	%
OPC	14.7 (0.2)	15.0 (0.6)	-1.9	17.5 (0.3)	17.7 (0.7)	-1.0	21.5 (0.3)	24.2 (0.5)	-11.2
GGBS	6.7 (0.2)	7.2 (0.1)	-7.6	11.7 (0.2)	11.5 (0.3)	2.4	20.5 (0.2)	21.8 (0.7)	-6.3
FA	1.0 (0.1)	1.0 (0.0)	1.2	1.9 (0.2)	2.2 (0.1)	-14.4	6.3 (0.3)	4.9 (0.1)	30.2
FCC	0.8 (0.1)	0.8 (0.1)	4.4	2.7 (0.2)	2.6 (0.1)	3.3	11.2 (0.3)	10.2 (0.3)	10.3
CW	1.9 (0.1)	1.9 (0.1)	-0.4	2.6 (0.1)	2.7 (0.0)	-6.0	7.0 (0.4)	5.8 (0.4)	22.3

Table 4. ANC results obtained via the 'combined-pH assay', C, and the 'single-pH assay', S, (standard deviation in parentheses) and the % difference between these values as calculated by Equation 1 (see text). The values listed correspond to the mean of three experiments.

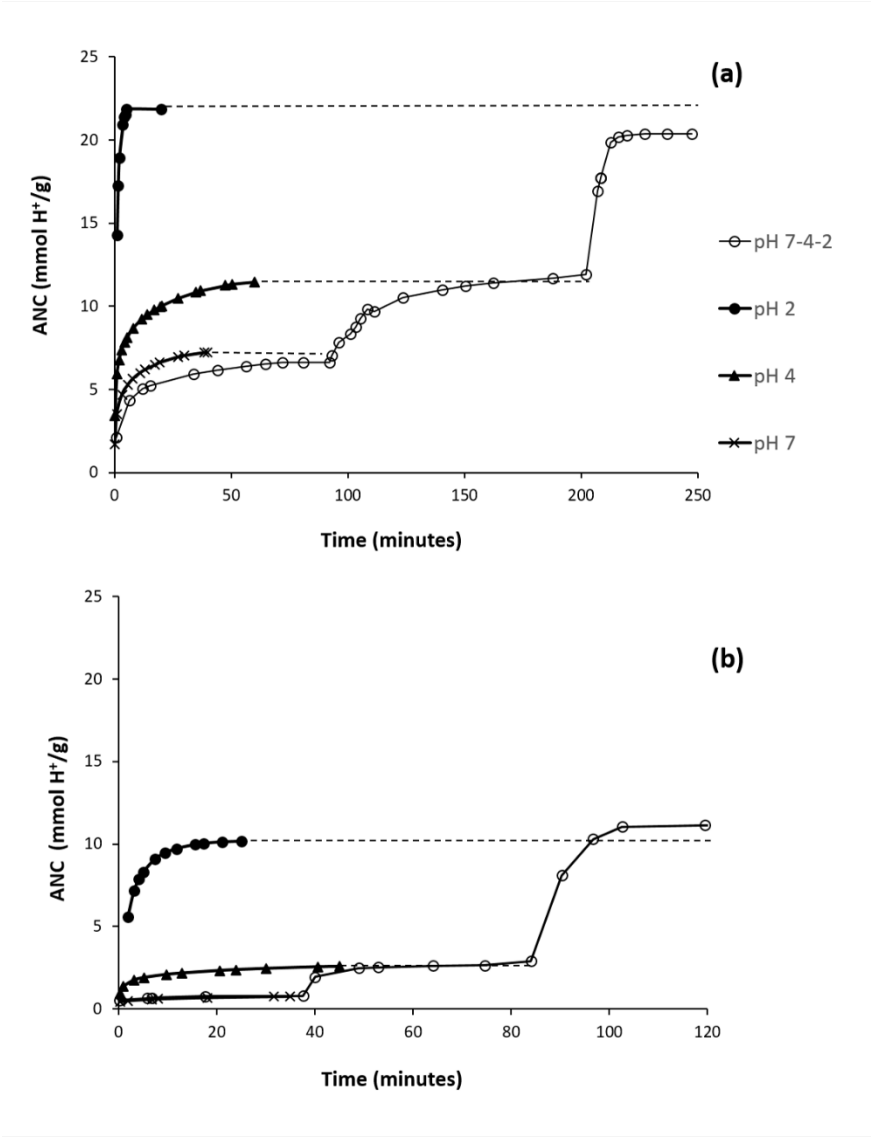

Fig. 2 ANC results obtained via the 'combined-pH assay' (pH 7-4-2) and the 'single-pH assay' (pH 2, pH 4 and pH 7) for **(a)** GGBS and **(b)** FCC samples.

OPC and GGBS behaved similarly in the two assays; ANC values obtained by the 'single-pH assay' were slightly superior to the ANC values obtained by the 'combined-pH assay' method, especially for pH 2. This difference can be attributed to the fact that in the 'combined-pH assay', addition of acid to pH 2 was initiated on a sample that had been previously attacked at pH 4 and 7. Conversely, the 'single-pH assay' for pH 2 required a high dose of acid at the

beginning of the test, and probably in these conditions there was a small excess of acid added. In any case, the ANC values obtained from both of these methods were very similar.

Results obtained for FA, FCC and CW samples at pH 7 were almost identical for the two methods. The differences were very small and we attribute the change of sign in the values of the percentage differences to natural experimental oscillations.

The same conclusions was drawn for ANC values obtained at pH 4 for these samples, although in these cases the percentage differences were somewhat larger.

However, clear differences between the test results at pH 2 were observed. In these cases, the ANC values for FA, FCC and CW samples by the 'combined-pH assay' were higher than the values obtained by the 'single-pH assay'. It is likely that the previous acid attack at pH 7 and 4 partially destroyed the matrix, and as more acid was added to bring the pH to 2 the reaction progressed to a greater extent than that observed in the 'single-pH assay'. Spent time for the 'combined-pH assay' was more than 100 min, while it took less than 25 min to complete the 'single-pH assay' at pH 2 (see Figs. 1 and 2). However, the determination of ANC values by the 'combined-pH assay' let to avoid the intermediate steps: cleaning of beaker, restoring the titration system and weighing of solid sample. Additionally, the consumption of acid is reduced.

Despite these differences, results from the 'combined-pH assay' show that it is possible to determine the ANC of a sample in a single test thereby saving time and chemical reagents.

3.2. Mass loss/consumed acid studies

Mass loss monitoring (ML) of monolithic specimens (1 × 1 × 6 cm prismatic shape) was carried out over 120 h. In this experiment, a pH of 2 was maintained by the addition of 1 M HNO_3, and consumed acid (CA) was recorded prior to mass measurements. A plot of added acid versus time and a plot of mass versus time are presented in Fig. 3. The acid added increased over time

280 (Fig. 3a) as a consequence of its continuous reaction with the alkaline matrix of the specimens.
281 In general, the trend we observed was similar to that from the ANC studies. Thus, the OPC
282 sample consumed 78 mL of acid solution, GGBS consumed 60 mL, and FCC and FA consumed
283 significantly lower amounts: 32 and 16 mL, respectively. Curiously, the CW sample consumed a
284 large amount of acid solution (54 mL) over 120 h, whereas in the ANC studies the quantity of
285 mmol H^+/g required was similar to that for the FA sample. This behaviour can be explained in
286 terms of cohesiveness of the samples. As will be described further in section 3.3, the sample
287 showed many cracks and the acid solution penetrated into the specimen. Under these
288 conditions, the surface attack was higher and consequently the CA increased strongly.

289 Every time the acid volume was recorded, the specimen was extracted from the beaker and
290 weighed. The trend observed for the mass (Fig. 3b) was similar to that found in the CA study.
291 The OPC specimen had a ML of 16% after 120 h, and had a ML greater than 6% after only 20
292 min. The FA sample showed the lowest ML at the end of the process: 2%. This behaviour
293 suggested that the low degree acid attack on the matrix developed by means alkali activation
294 of FA as a consequence of the stability of the N-A-S-H gel formed during hydration. The CW
295 sample experienced a significant drop in its mass after 120 h (slightly less than 11%), which is
296 in accord with the CA sample. After 20 min, its ML of the CW sample was only 3%, similar to
297 the value found for the FCC sample. After this time, however, its ML increased notably, which
298 we attributed to the above mentioned cracking process in the prismatic specimen. When the
299 cracks were wide, part of the solid material was lost as small particles (less than 1 mm) and
300 consequently the acid consumption was higher than expected from the ANC test.

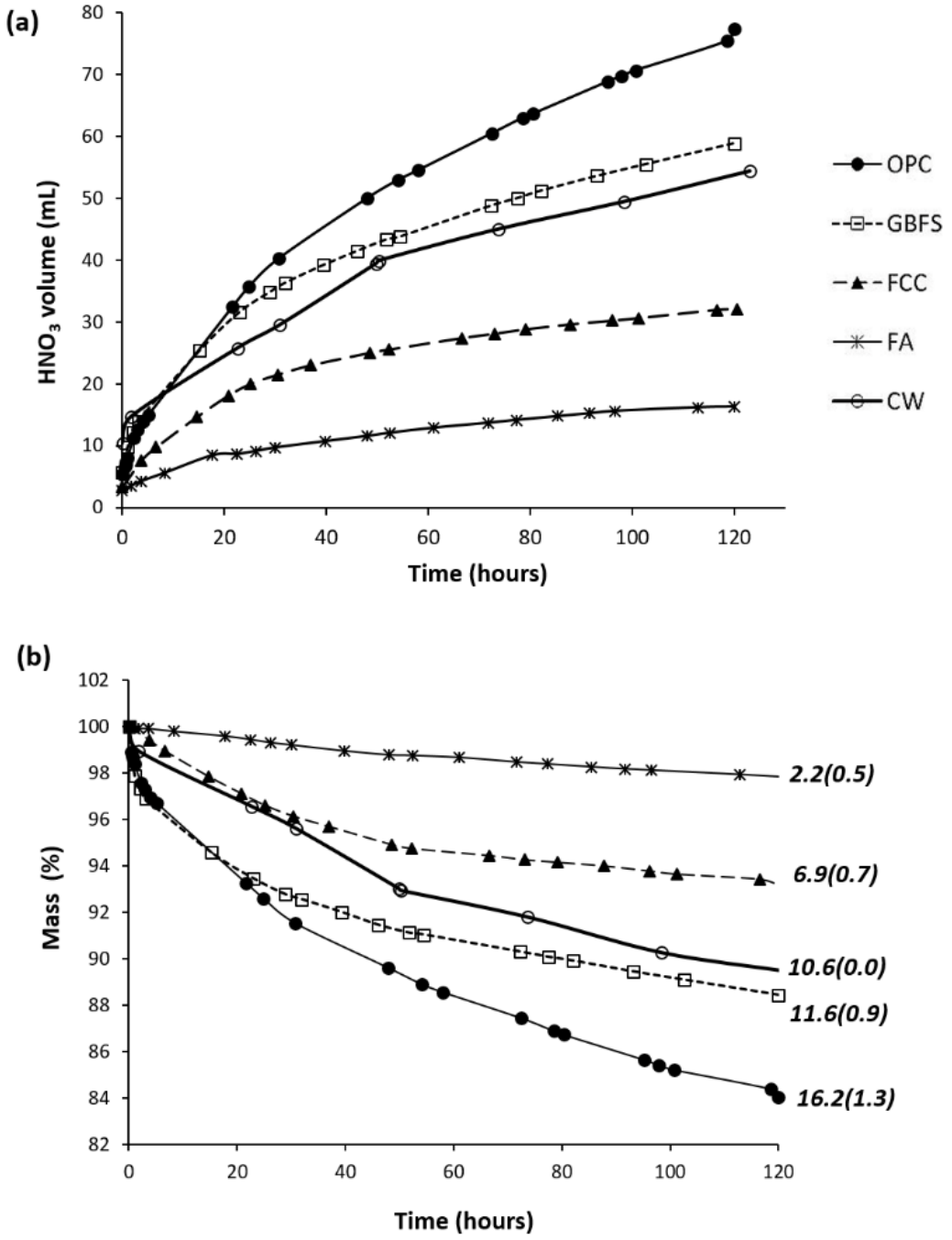

Fig. 3 (a) Amount of 1 M nitric acid added (mL) and **(b)** mass (%) versus time (h) for monolithic specimens of OPC and alkali-activated pastes. Mass loss percentages for 120 hours (ML) are given in Figure 3b (average values and standard deviations)

308 **Table 5** Parameters used to fit equations of relative mass versus time for the studied samples.

	Equations*	Time interval (hours)
OPC	$z = -0.0019\,x^2 + 0.289\,x + 98.688$	0 – 72
	$z = -0.0676\,x + 92.186$	72 – 120
GGBS	$z = -0.0032\,x^2 + 0.306\,x + 98.832$	0 – 72
	$z = -0.0676\,x + 92.186$	72 – 120
FA	$z = -0.0258\,x + 99.995$	0 – 48
	$z = -0.0137\,x + 99.447$	48 – 120
FCC	$z = -0.0012\,x^2 - 0.1646\,x + 99.994$	0 – 48
	$z = -0.0228\,x + 95.965$	48 – 120
CW	$z = -0.0006\,x^2 - 0.1558\,x + 99.643$	0 – 30
	$z = -0.0507\,x + 95.496$	30 – 120

309

310 **Table 5.** Fitting equations of relative mass versus time (z is mass in % and x is time in h).

311 * The shape of these curves makes it impossible to fit a single equation, thus separate

312 equations were used for each time interval.

313

314 *3.3. Optical microscopy studies*

315 Fig. 4 shows photographs obtained by optical microscopy from the surface and cross section of
316 each of the specimens after 120 h of acid attack. Freshly fractured specimens were sprayed
317 with a phenolphthalein solution to visualise the degree of acid penetration.

318 The surface of the OPC specimen (Fig. 4a) exhibited a light brown colour on its surface layer (to
319 a depth of 0.4 mm) with deep, it showed wide cracks (150–200 μm) and it was easily
320 removable. Under the surface layer, a grey layer (0.6 mm deep) was identified, in which the
321 phenolphthalein colour suggested a high neutralisation level (with a pH under 10). Finally, the
322 deepest layer was red due to acid attack that did not get neutralised completely. The GGBS
323 sample (Fig. 4b) showed a pattern similar to the OPC sample; in this case the first and second
324 layers were both 0.4 mm deep.

325 The FA sample (Fig. 4c) also had a cracked pattern, but in this case the cracks were much
326 thinner (20–80 μm) than those in the above mentioned samples (OPC and GGBS). In the cross
327 sectional image no evidence of cracking was observed. This is consistent with the high stability
328 of this sample when attacked by acid. The phenolphthalein treatment revealed that
329 neutralisation was achieved in the first 1.2 mm, however this neutralisation did not show
330 evidence of matrix damage.

331 The width for the cracks observed for the FCC sample (Fig. 4d) was intermediate between the
332 FA and OPC or GGBS samples. In the cross sectional image, three layers were also observed as
333 for OPC: the first layer showed a cracked pattern with a depth of 0.3 mm, the second layer (0.4
334 mm) was a whitish zone (colourless phenolphthalein) and the third layer corresponded to the
335 core that was not attacked.

336 Finally, the CW sample (Fig. 4e) had the thickest cracks (250–350 μm) and these cracks
337 penetrated deeply into the sample. This allowed for complete neutralisation of the sample
338 which was observable in the phenolphthalein treatment: a red colour was not identified in the
339 cross sectional image. This result is in agreement with the high acid consumption observed for
340 this sample. Internal zones of the CW paste specimen were attacked by the acid through these
341 large cracks. The mechanical stability of this sample was very poor, and some parts of it were
342 easily removed by hand.

343 According to these experiments, the FA specimens were the most resistant to acid attack,
344 followed by samples prepared with FCC. The specimens most susceptible to acid attacked were
345 those made from CW. OPC and GGBS samples gave similar results.

346

347

348

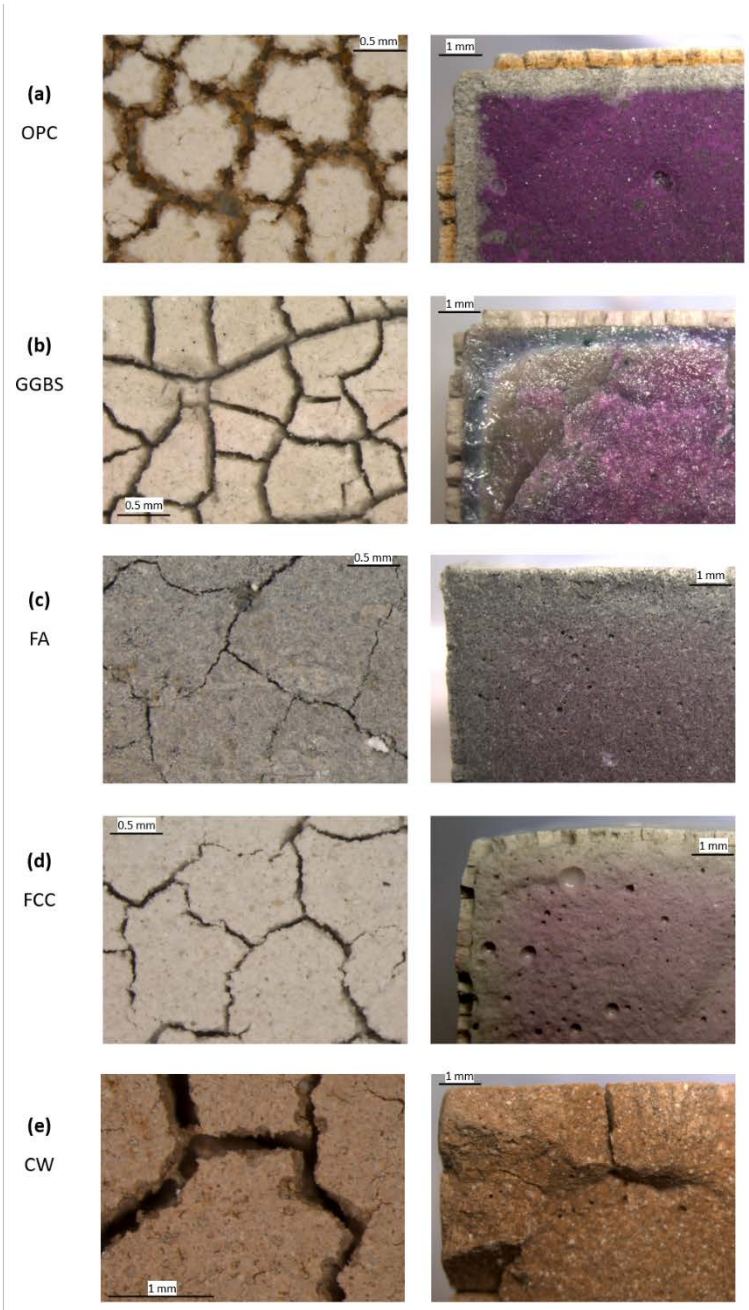

Fig. 4 Photographs taken by optical microscopy of **(a)** OPC, **(b)** GGBS, **(c)** FA, **(d)** FCC and **(e)** CW from the surface and a cross section of the monolithic specimens attacked by 1 M nitric acid for 120 h.

3.4. SEM studies

Micrographs and elemental mappings on the polished cross sections of the attacked samples are showed in Figs. 5–9. We emphasise that it was impossible to analyse the outermost layer

356 of the OPC and CW samples by SEM because the outermost layer was lost during the polishing
357 process used to prepare samples for SEM.

358 Fig. 5 shows the backscattered micrograph from the OPC sample and the mapping distribution
359 of calcium. In this case, the outermost layer was not present, and there is a small change in the
360 calcium concentration. The external layer had less calcium due to leaching into the acid
361 medium. The change in pH was perfectly characterised by phenolphthalein treatment (Fig. 4a).
362 This means that the neutralisation process took place in this zone, however the leaching of
363 calcium was less important.

364

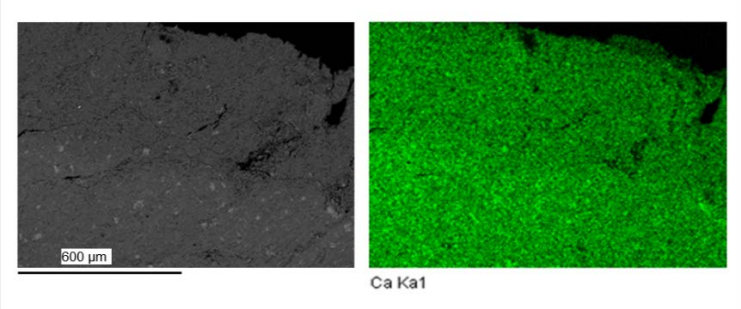

365

366 **Fig. 5** Backscattered micrograph and mapping distribution of calcium for the OPC sample.

367

368 Micrographs for the GGBS samples are shown in Fig. 6. In this case, the outermost layer was
369 maintained, and a clear attack zone is displayed. For this layer, calcium was completely
370 leached leaving behind silicon as the main element. This means that a silica gel based layer was
371 formed, which resulted in large cracks. Aluminium was also partially leached from this external
372 layer.

373 For the FA sample, a negligible amount of leaching of sodium and aluminium was observed,
374 suggesting the binding matrix was quite stable (Fig. 7) and that N-A-S-H gels have good
375 resistance to acid. Conversely, in the FCC sample (Fig. 8) the external attacked layer leached

significant amounts of sodium, leaving behind the aluminium and silicon, suggesting that the N-A-S-H gel decomposed yielding a mixture of silica and alumina gels.

Finally, for the CW sample a strong attack was characterised (Fig. 9), and a large leached layer was easily identified by calcium and aluminium map distributions.

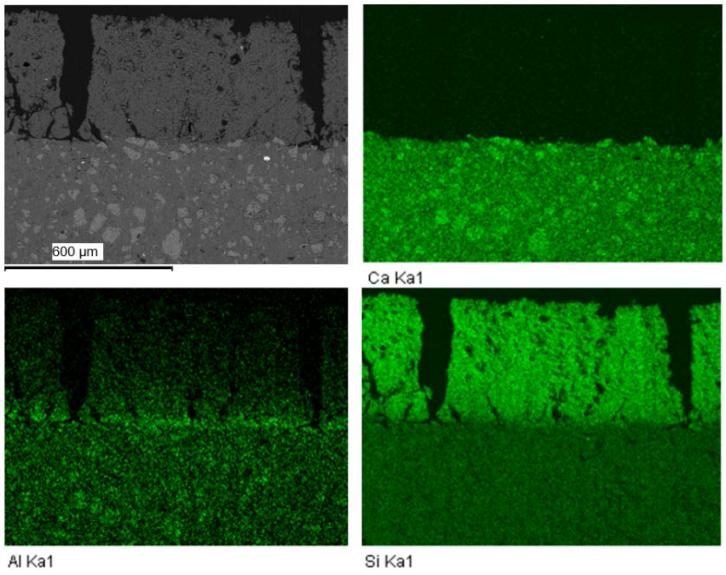

Fig. 6 Backscattered micrograph and mapping distribution of calcium, aluminium and silicon for the GGBS sample.

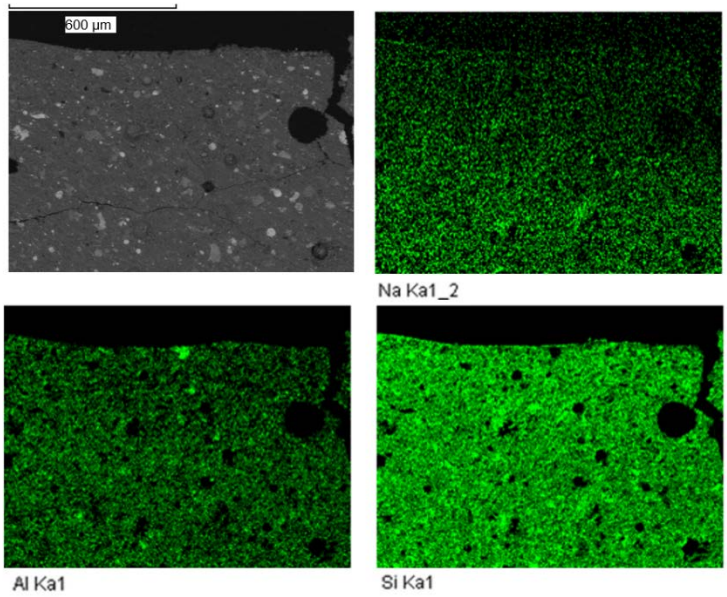

Fig. 7 Backscattered micrograph and mapping distribution of sodium, aluminium and silicon for the FA sample.

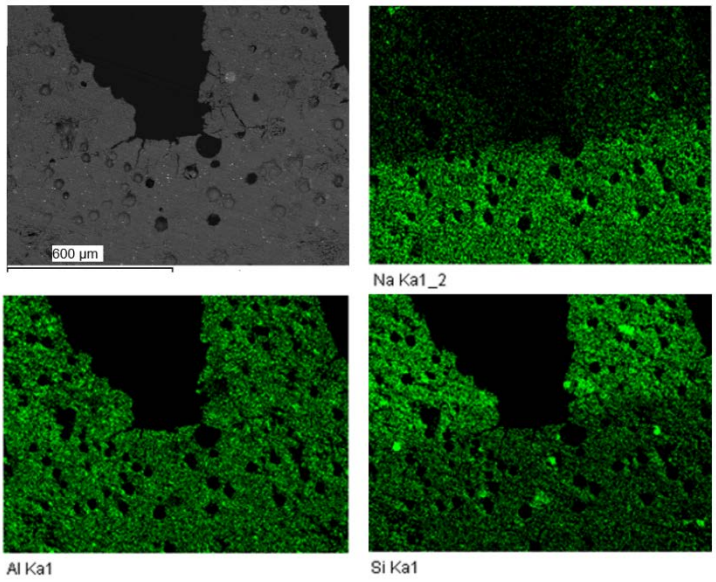

386

387 **Fig. 8** Backscattered micrograph and mapping distribution of sodium, aluminium and silicon for
388 the FCC sample.

389

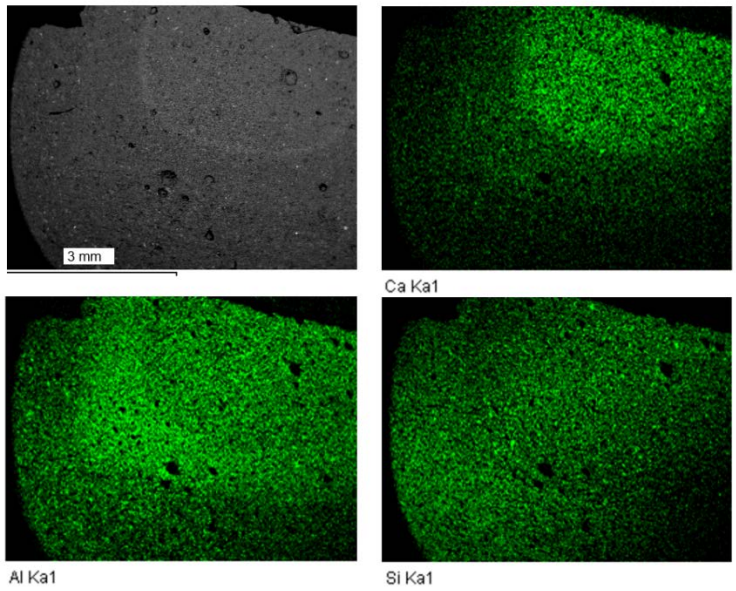

390

391 **Fig. 9** Backscattered micrograph and mapping distribution of calcium, aluminium and silicon
392 for the CW sample.

393

394

395

4. Conclusions

Durability tests are generally tedious and time consuming. Here, two rapid tests to evaluate resistance to acid attack for alkali-activated samples have been outlined: acid neutralisation capacity (ANC) monitoring and mass loss/consumed acid (ML/CA) monitoring.

These two methods have been used to analyse resistance to acid attack for some alkali-activated pastes prepared from GGBS, FA, FCC and CW. Their behaviour has been compared to hardened OPC pastes.

In general, ANC values are directly related to the Ca content of the samples, except for FCC. The higher the content of Ca in the samples, the higher the ANC value. The different behaviour of FCC may be due to the different curing conditions used for this sample relative to other alkali-activated materials containing low amounts of Ca (FA and CW). We have obtained solved equations for ANC versus time for each of the samples at pH 7, 4 and 2 in order to predict the behaviour against acid attack for a given sample.

Based on the ANC methodology, a new method called ‘combined-pH assay’ was proposed. This assay involved determining the ANC of a sample at different pH values using the same aliquot. Results showed that it is possible to determine the ANC of a sample in a single test thereby saving chemical reagents and total processing time.

A new method, ML/CA, based on nitric acid attack (addition of a 1 M solution to maintain a pH of 2) was applied. Observations after 120 h of treatment (CA, ML and microscopic features) on monolithic specimens showed that the FA samples were the most resistant to acid attack, followed closely by the FCC sample and then the OPC and GGBS samples. Finally, the CW samples were the most susceptible to acid attack due to its low mechanical stability.

418 Further research is required in order to apply these methods to mortars and concrete, taking
419 into account the changes required in the size/shape of the samples and the possibility of the
420 reaction of aggregates in acid medium.

421

422 **References**

423 1. C. Shi, P.V. Krivenko, D. Roy, Alkali-activated cements and concretes, Taylor&Francis
424 (Oxon,UK), 2006.
425 2. J.L. Provis, J.S.J. van Deventer, Geopolymers. Structure, processing, properties and
426 industrial applications, Woodhead Publishing Limited (Cambridge, UK), 2009.
427 3. F. Pacheco-Torgal, J. Castro-Gomes, S. Jalali, Alkali-activated binders: A review. Part I.
428 Historical background, terminology, reaction mechanisms and hydration products,
429 Constr. Build. Mater. 22 (2008) 1305–1314. doi:10.1016/j.conbuildmat.2007.10.015
430 4. F. Pacheco-Torgal, J. Castro-Gomes, S. Jalali, Alkali-activated binders: A review. Part II.
431 About materials and binders manufacture, Constr. Build. Mater. 22 (2008) 1315–1322.
432 doi:10.1016/j.conbuildmat.2007.03.019
433 5. C. Shi, A. Fernández Jiménez, A. Palomo, New cements for the 21st century: The
434 pursuit of an alternative to Portland cement, Cement Concrete Res. 41 (2011) 750–
435 763. doi:10.1016/j.cemconres.2011.03.016
436 6. J.L. Provis, A. Palomo, C. Shi, Advances in understanding alkali-activated materials,
437 Cement Concrete Res. 78 (2015) 110–125. doi.org/10.1016/j.cemconres.2015.04.013
438 7. M.M. Tashima, J.L. Akasaki, V.N. Castaldelli, L. Soriano, J. Monzó, J. Payá, M.V.
439 Borrachero, New geopolymeric binder based on fluid catalytic cracking catalyst residue
440 (FCC), Mater. Lett. 80 (2012) 50–52. doi:10.1016/j.matlet.2012.04.051
441 8. M.M. Tashima, J.L. Akasaki, J.L.P. Melges, L. Soriano, J. Monzó, J. Payá, M.V.
442 Borrachero, Alkali activated materials based on fluid catalytic cracking catalyst residue

(FCC): Influence of SiO_2/Na_2O and H_2O/FCC ratio on mechanical strength and microstructure, Fuel. 108 (2013) 833–839. doi.org/10.1016/j.fuel.2013.02.052

9. E.D. Rodríguez, S.A. Bernal, J.L. Provis, J.D. Gehman, J.M. Monzó, J. Payá, Borrachero M.V., Geopolymers based on spent catalyst residue from a fluid catalytic cracking (FCC) process, Fuel. 109 (2013) 493–502. doi.org/10.1016/j.fuel.2013.02.053
10. L. Reig, M.M. Tashima, L. Soriano, M.V. Borrachero, J. Monzó, J. Payá, Alkaline activation of ceramic waste materials, Waste Biomass Valor. 4 (2013) 729–736. doi 10.1007/s12649-013-9197-z
11. L. Reig, M.M. Tashima, M.V. Borrachero, J. Monzó, C.R. Cheeseman, J. Payá, Properties and microstructure of alkali-activated red clay brick waste, Constr. Build. Mater. 43 (2013) 98–106. doi.org/10.1016/j.conbuildmat.2013.01.031
12. V. Zivica, A. Bajza, Acidic attack of cement based materials – a review. Part 1. Principle of acidic attack, Constr. Build. Mater. 15 (2001) 331–340.
13. V. Zivica, A. Bajza, Acidic attack of cement based materials – a review. Part 2. Factors of rate of acidic attack and protective measures, Constr. Build. Mater. 16 (2002) 215–222.
14. V. Zivica, Acidic attack of cement based materials – a review. Part 3. Research and test methods, Constr. Build. Mater. 18 (2004) 683–688. doi:10.1016/j.conbuildmat.2004.04.030
15. T. Gutberlet, H. Hilbig, R.E. Beddoe, Acid attack on hydrated cement – Effect of mineral acids on the degradation process, Cement Concrete Res. 74 (2015) 35–43. doi.org/10.1016/j.cemconres.2015.03.011
16. R.E. Beddoe, H.W. Dorner, Modelling acid attack on concrete: Part I. The essential mechanisms, Cement Concrete Res. 35 (2005) 2333–2339. doi:10.1016/j.cemconres.2005.04.002

17. F. Pacheco-Torgal, Z. Abdollahnejad, A.F. Camões, M. Jamshidi, Y. Ding, Durability of alkali-activated binders: A clear advantage over Portland cement or an unproven issue?, Constr. Build. Mater. 30 (2012) 400–405. doi:10.1016/j.conbuildmat.2011.12.017
18. C. Shi, J.A. Stegemann, Acid corrosion resistance of different cementing materials, Cement Concrete Res. 30 (2000) 803–808.
19. T. Bakharev, J.G. Sanjayan, Y.B. Cheng, Resistance of alkali-activated slag concrete to acid attack, Cement Concrete Res. 3 (2003) 1607–1611. doi:10.1016/S0008-8846(03)00125-X
20. T. Bakharev, Resistance of geopolymer materials to acid attack, Cement Concrete Res. 35 (2005) 658–670. doi:10.1016/j.cemconres.2004.06.005
21. A. Fernandez-Jiménez, I. García-Lodeiro, A. Palomo, Durability of alkali-activated fly ash cementitious materials, J. Mater. Sci. 42 (2007) 3055–3065. doi 10.1007/s10853-006-0584-8
22. A. Allahverdi, F. Škvára, Nitric acid attack on hardened paste of geopolymeric cements Part 1, Ceram-Silikáty. 45 (2001) 81–88.
23. A. Allahverdi, F. Škvára, Nitric acid attack on hardened paste of geopolymeric cements Part 2, Ceram-Silikáty. 45 (2001) 143–149.
24. EA NEN 7371:2004, Leaching characteristics of granular building and waste materials. The determination of the availability of inorganic components for leaching. 'The maximum availability leaching test', Environment Agency, Version 1.0, April 2005.